Electronic Supplementary Material (ESI) for Dalton Transactions.

Supporting Information

Highly Stable Halide Perovskites for Photocatalysis via Multi-dimensional Structure Design and In-situ Phase Transition†

Yiqin Gong,[a‡] Fan Ye,[b‡] Qiliang Zhu,[a] Wei Yan,[a] Jianhua Shen,[a] Kan-Hao Xue,*[b] Yihua Zhu,*[a] Chunzhong Li[a]*

[a.] Shanghai Engineering Research Centre of Hierarchical Nanomaterials, Key Laboratory for Ultrafine Materials of Ministry of Education, School of Materials Science and Engineering, East China University of Science and Technology, Shanghai 200237, China.

[b.] School of Optical and Electronic Information, Wuhan National Laboratory for Optoelectronics, Huazhong University of Science and Technology, Wuhan 430074, China.

E-mail: jianhuashen@ecust.edu.cn; xkh@hust.edu.cn; yhzhu@ecust.edu.cn.

[‡] *These authors contributed equally to this work.*

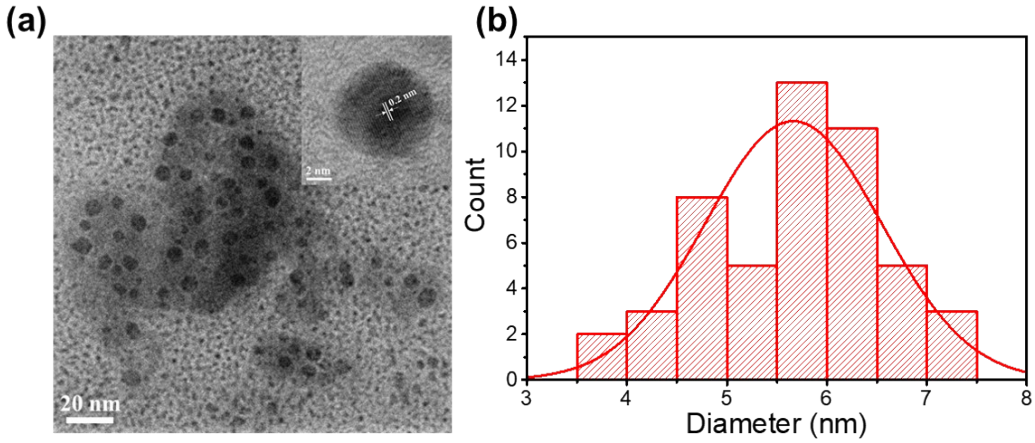

Fig. S1 (a) TEM image of $CsPbBr_3$ QDs. (b) Size distribution of $CsPbBr_3$ QDs.

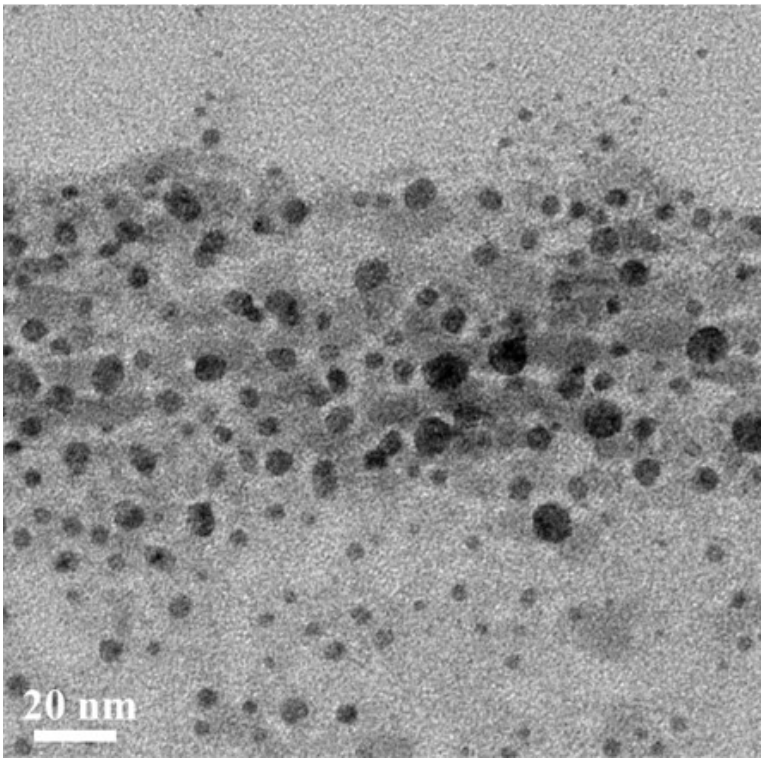

Fig. S2 TEM image of 0.1 PEABr sample.

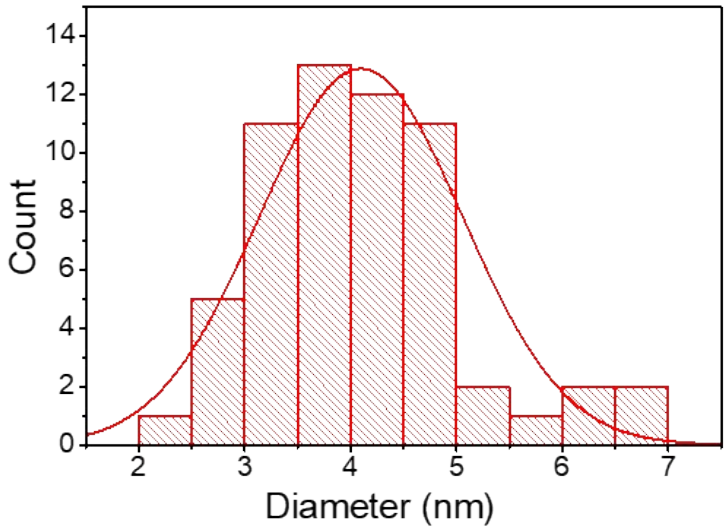

Fig. S3 Size distribution of 0.3 PEABr sample.

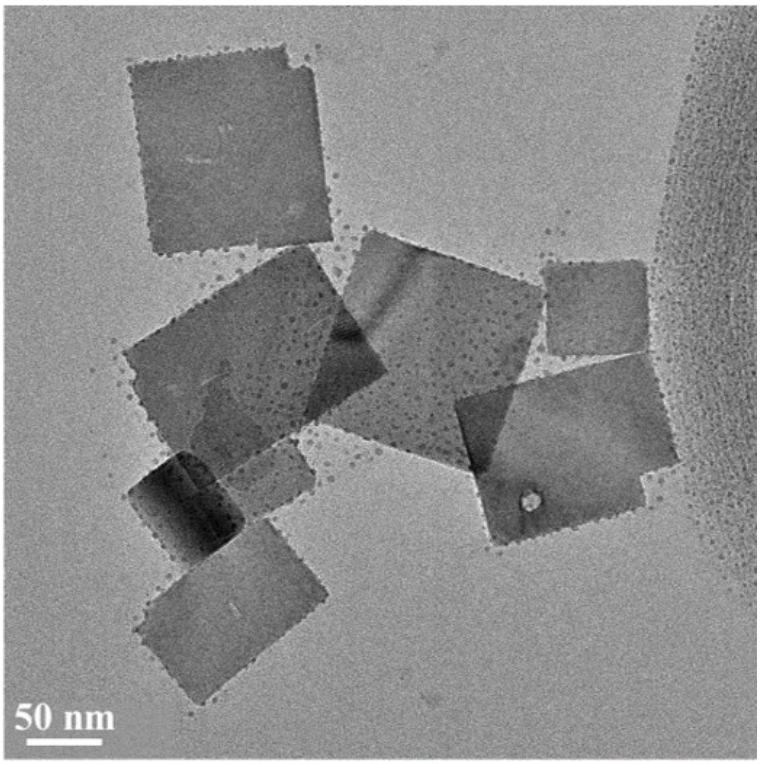

Fig. S4 TEM image of 0.5 PEABr sample.

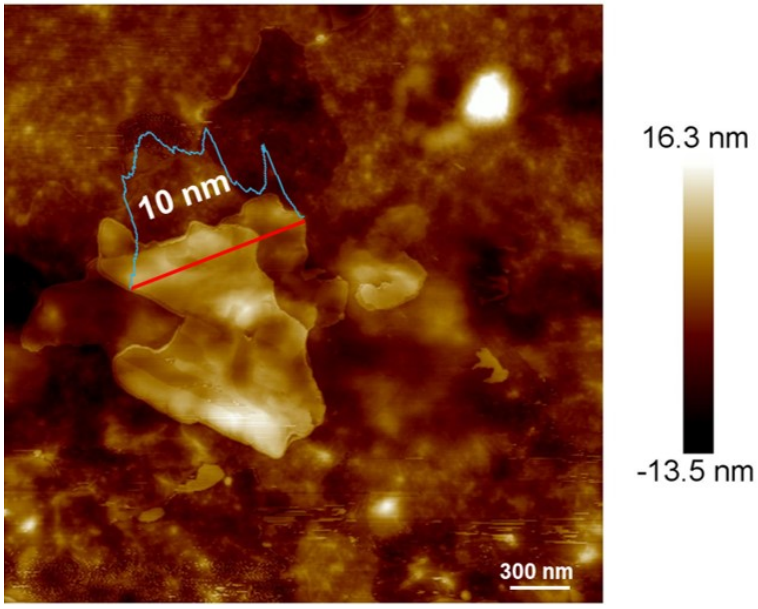

Fig. S5 AFM images of 0.5 PEABr sample.

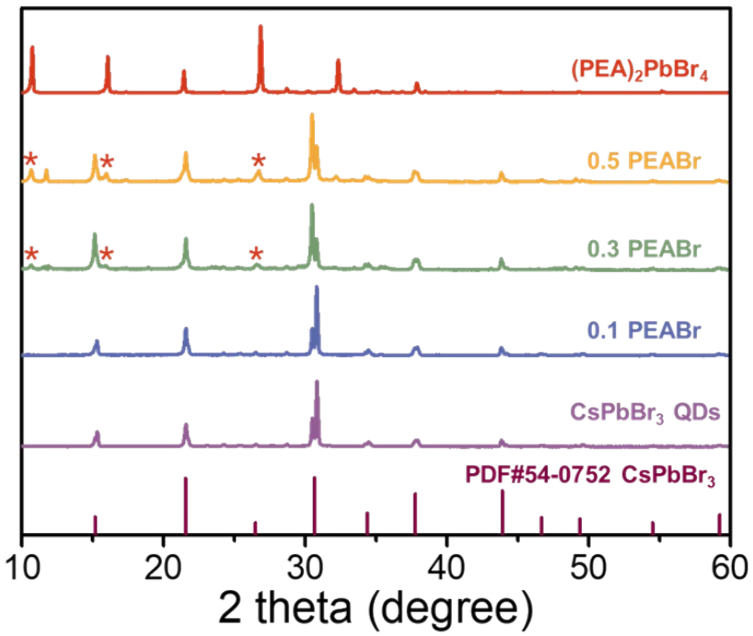

Fig. S6 XRD pattern of $CsPbBr_3$ QDs, 0.1 PEABr sample, 0.3 PEABr sample, 0.5 PEABr sample, 2D $(PEA)_2PbBr_4$ sample.

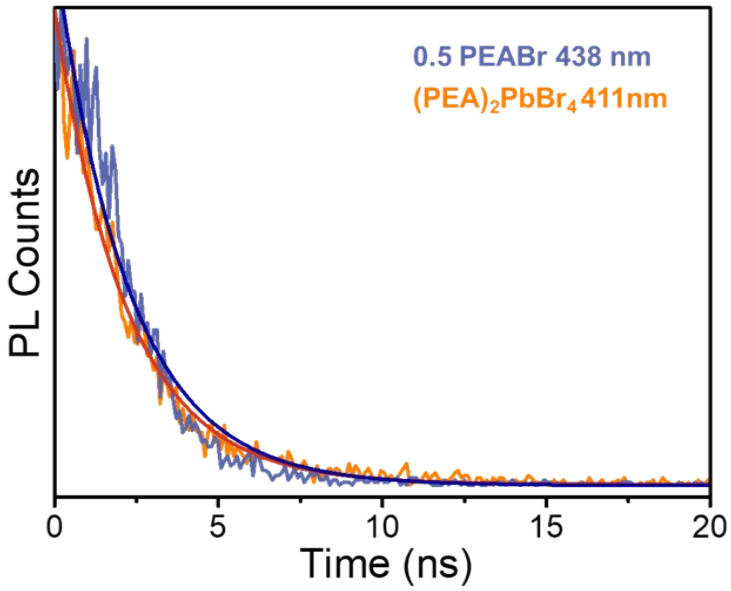

Fig. S7 Time-resolved PL spectra of 0.5 PEABr sample and 2D $(PEA)_2PbBr_4$ sample.

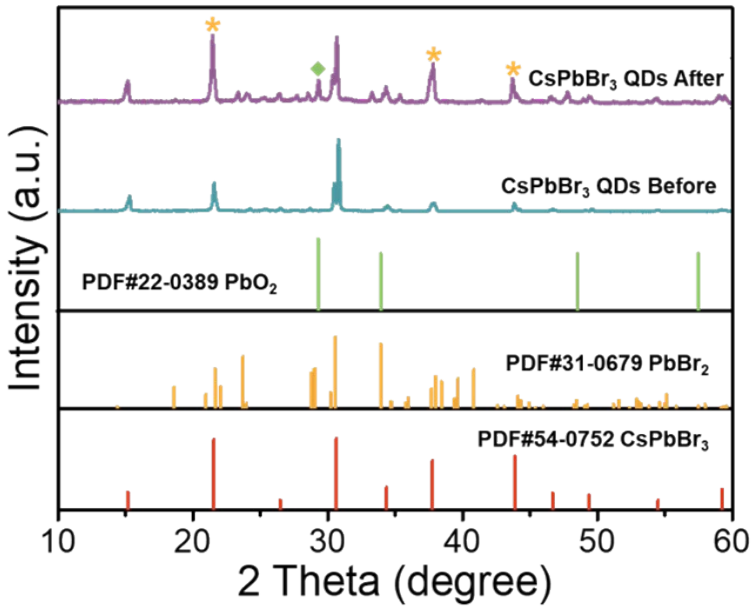

Fig. S8 XRD patterns of $CsPbBr_3$ QDs sample before and after photocatalytic reaction.

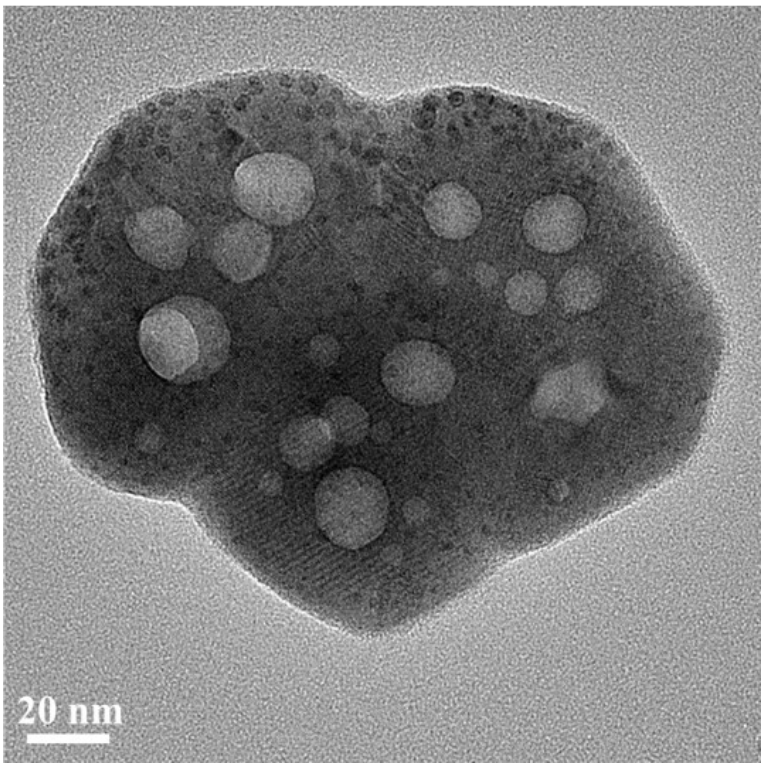

Fig. S9 TEM image of $CsPbBr_3$ QDs sample after reaction.

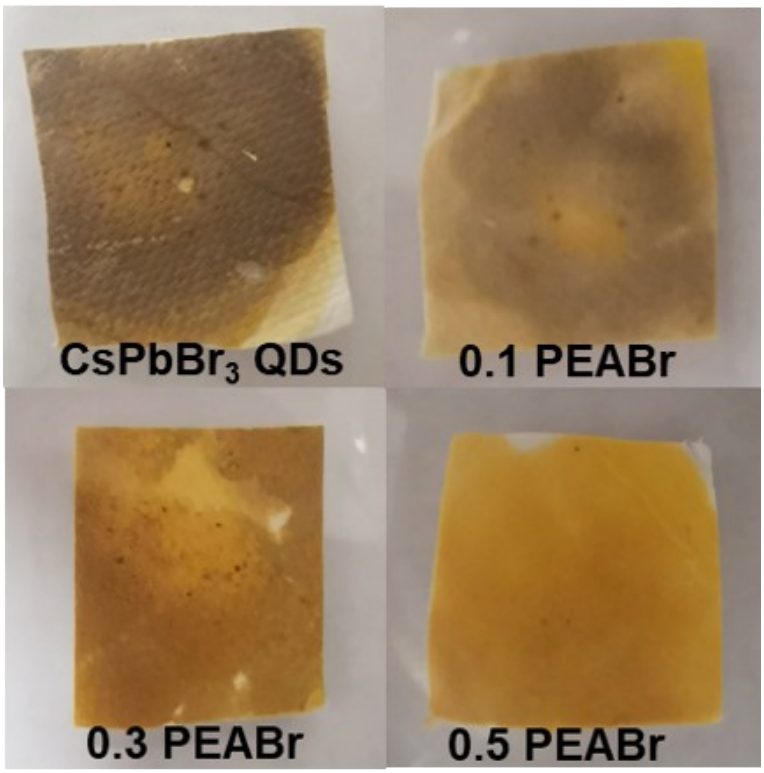

Fig. S10 Optical photographs of samples after photocatalytic reaction.

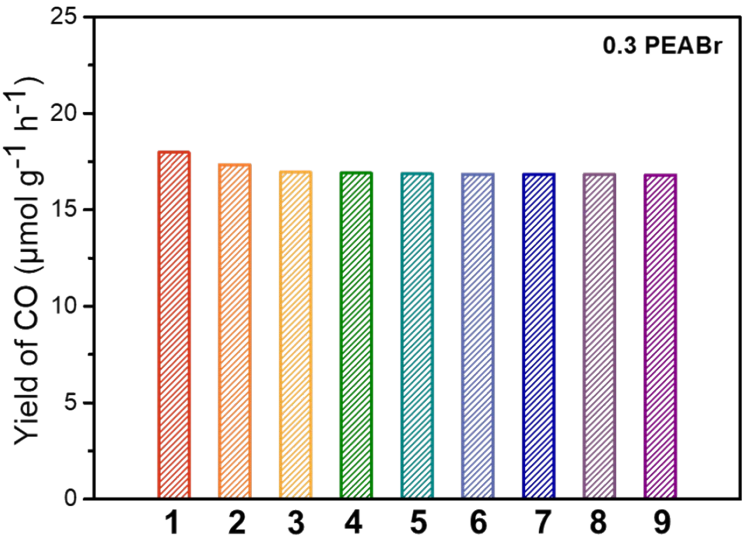

Fig. S11 Yield of CO after 3 h photochemical reaction of 0.3 PEABr sample as photocatalysts after 9 cycles.

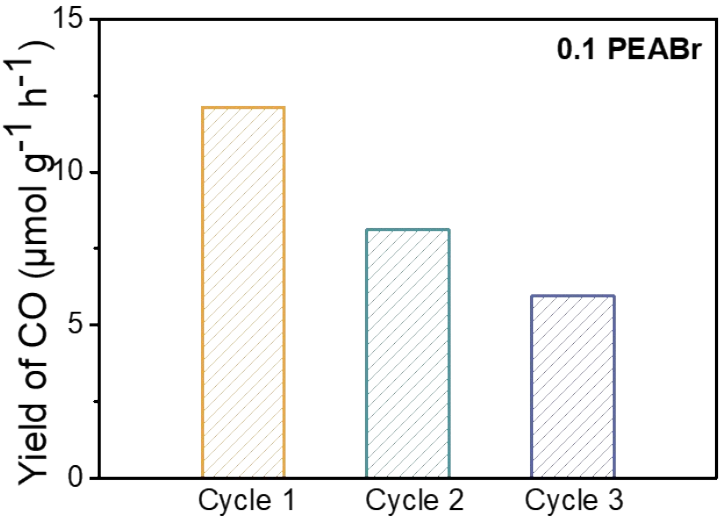

Fig. S12 Yield of the CO after 3 h photochemical reaction of 0.1 PEABr sample as photocatalysts after 3 cycles.

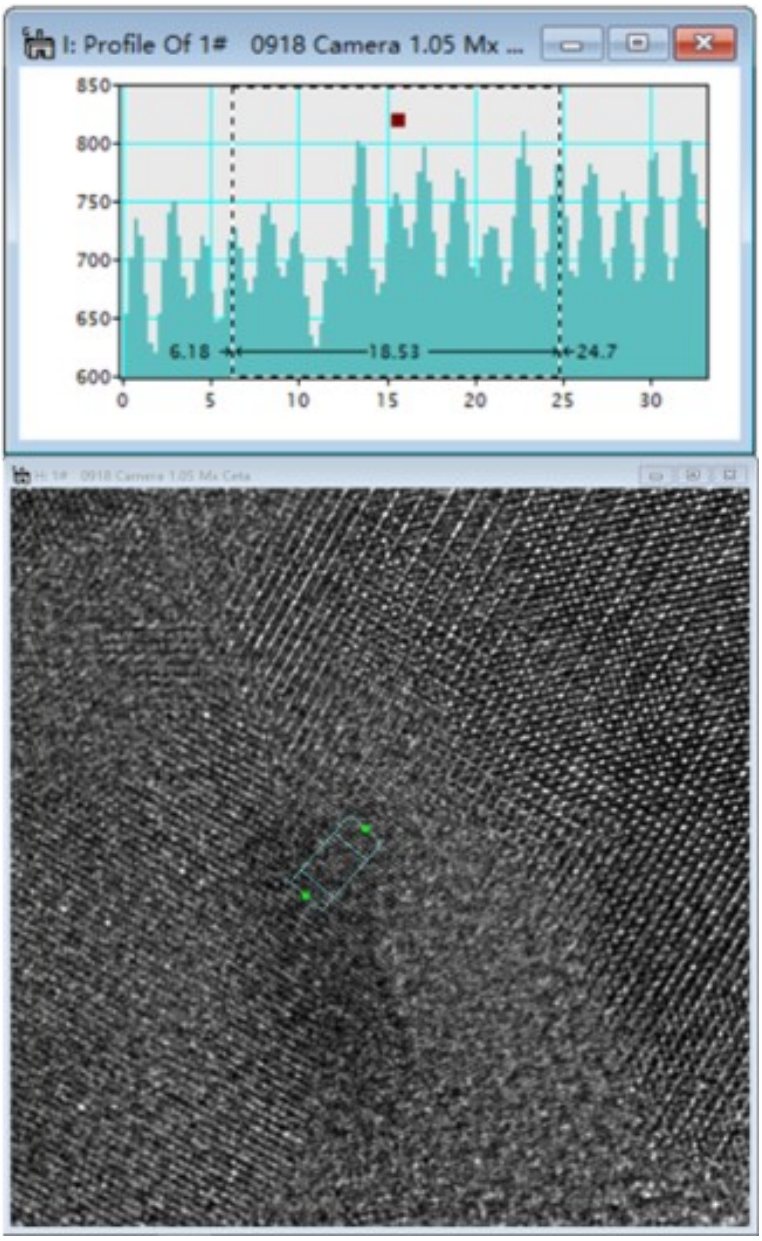

Fig. S13 Partly enlarged area of Figure 4a (marked with yellow).

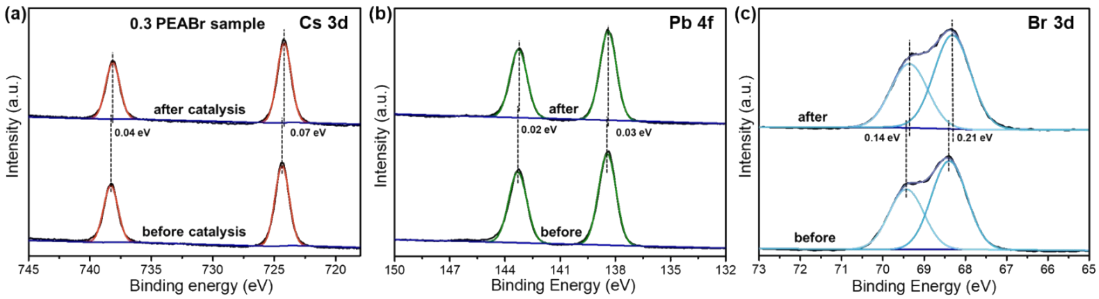

Fig. S14 High-resolution XPS spectra of Cs 3d, Pb 4f and Br 3d of 0.3 PEABr sample before and after catalysis.

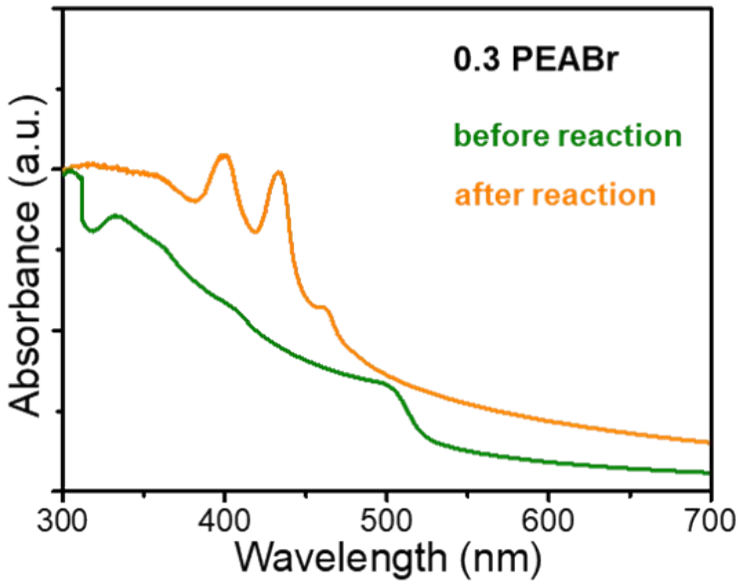

Fig. S15 Absorbance spectra of 0.3 PEABr sample before and after reaction.

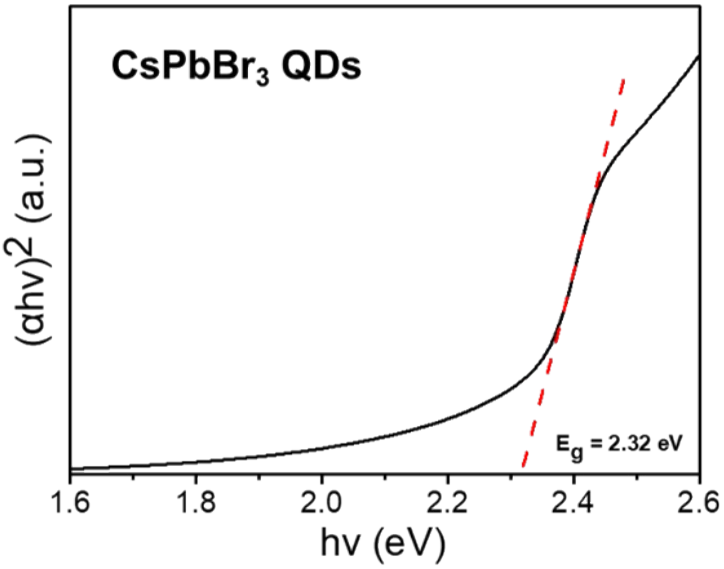

Fig. S16 Tauc plots of $CsPbBr_3$ QDs sample.

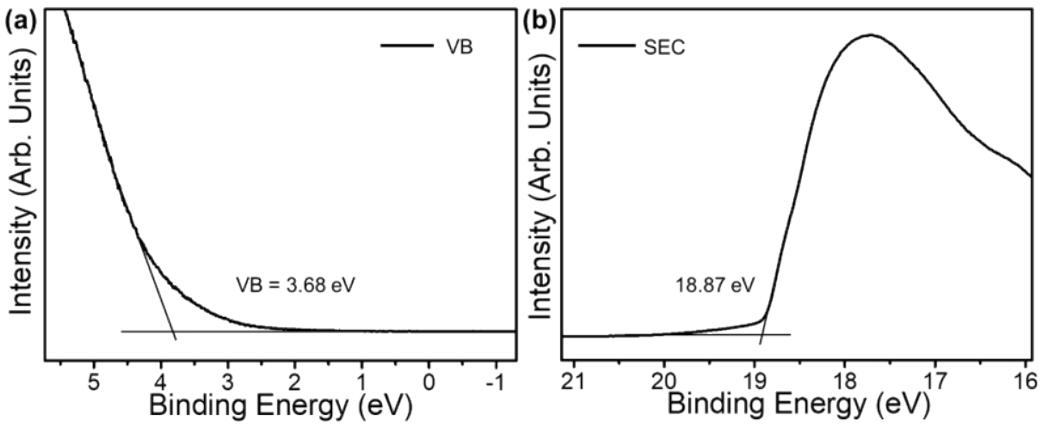

Fig. S17 UPS spectra of $CsPbBr_3$ QDs. (a) shows valence band maximum. (b)shows the spectra close to the Fermi edge.

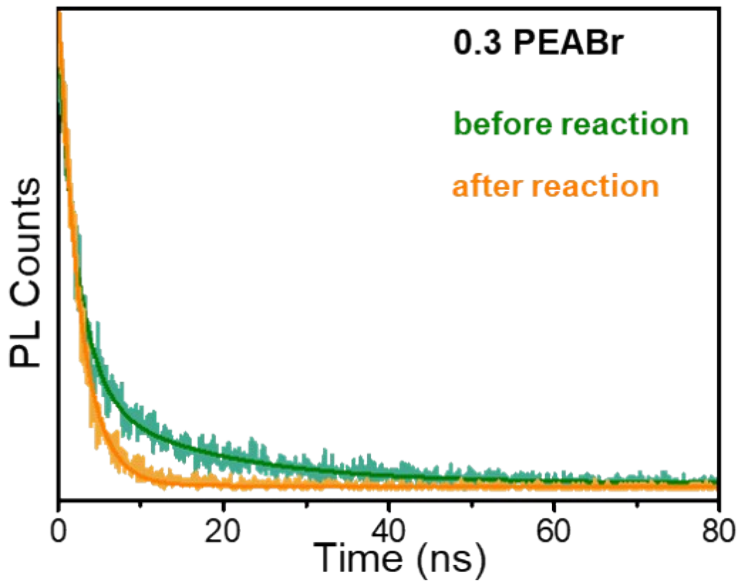

Fig. S18 Time-resolved PL spectra of 0.3 PEABr sample before and after reaction.

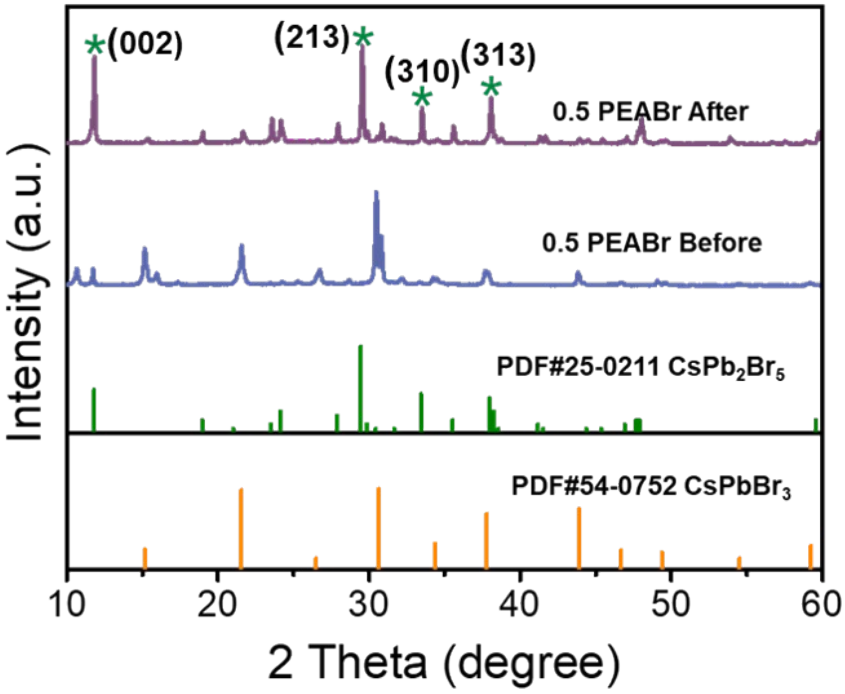

Fig. S19 XRD patterns of 0.5 PEABr sample before and after photocatalytic reaction.

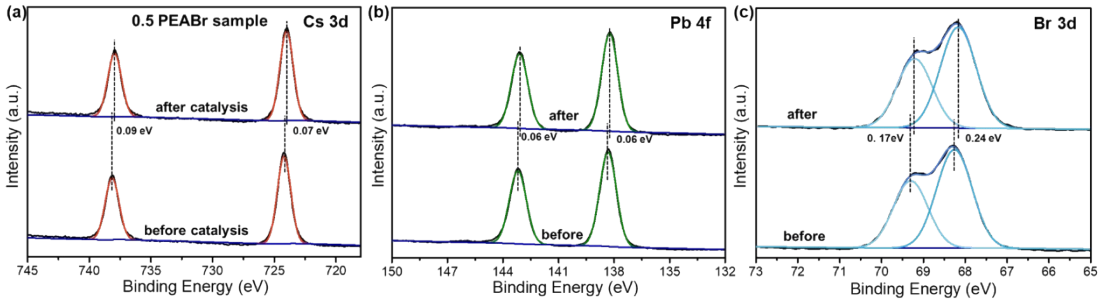

Fig. S20 High-resolution XPS spectra of Cs 3d, Pb 4f and Br 3d of 0.5 PEABr sample before and after catalysis.

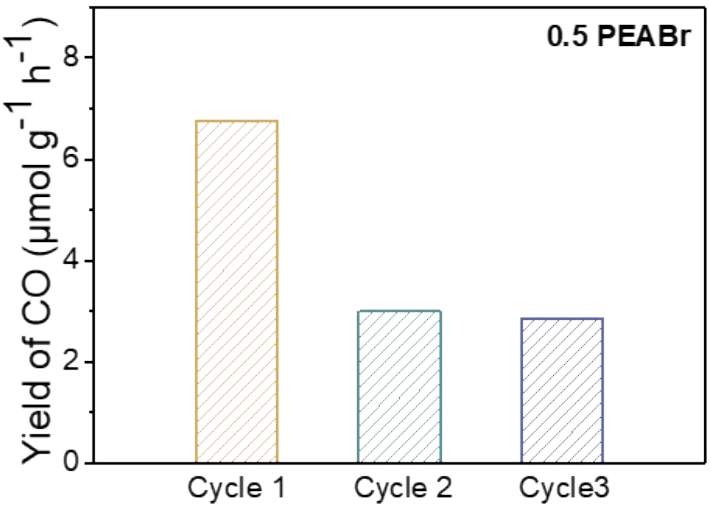

Fig. S21 Yield of the CO after 3 h photochemical reaction of 0.5 PEABr sample as photocatalysts after 3 cycles.

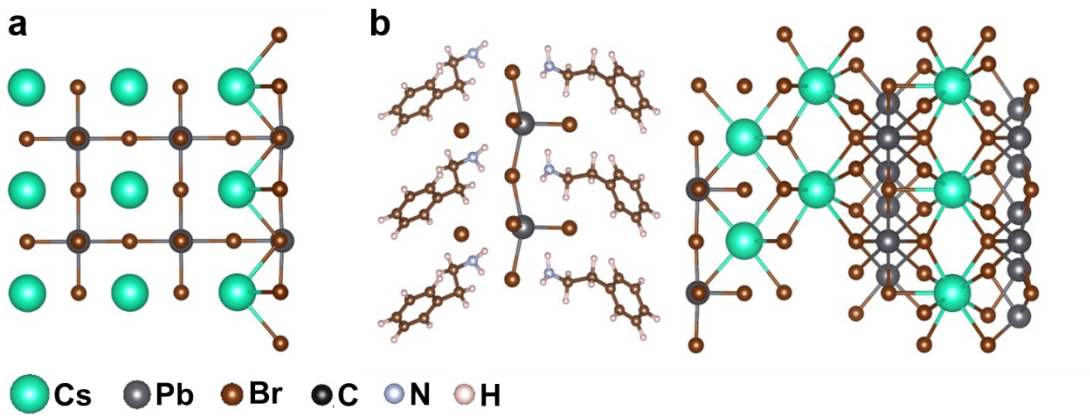

Fig. S22 Schematic structure of (a) $CsPbBr_3$ QDs and (b) $(PEA)_2PbBr_4$ NSs/$CsPbBr_3$ QDs/$CsPb_2Br_5$ NSs.

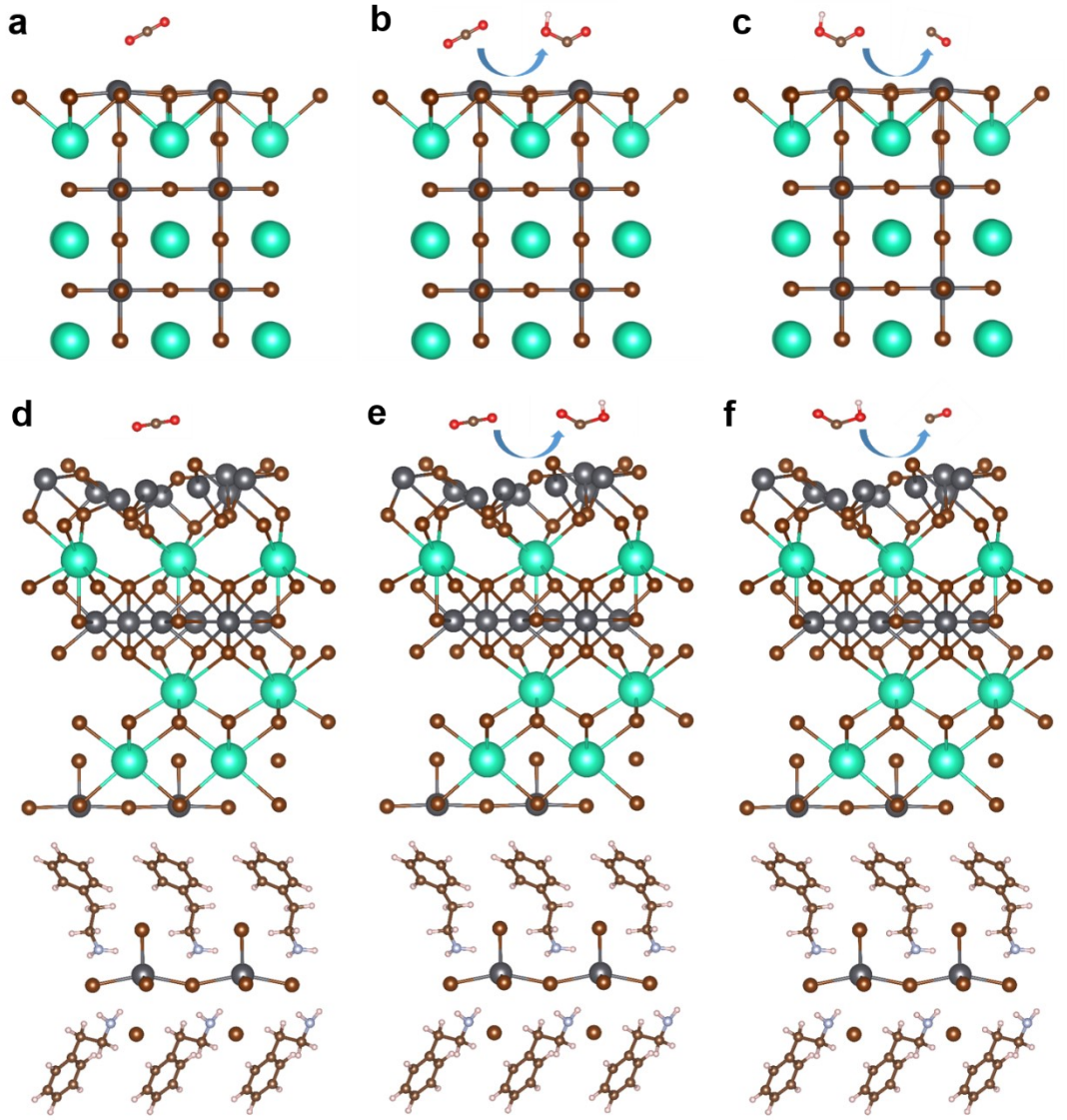

Fig. S23 Simulated process of CO_2 adsorbed on (a) $CsPbBr_3$ QDs and (d) $(PEA)_2PbBr_4$ NSs/$CsPbBr_3$ QDs/$CsPb_2Br_5$ NSs. (b, e) The conversion process of CO_2 to *COOH. (c, f) The conversion process of *COOH to *CO.

Table S1 Fitted data by biexponential decay kinetics of PL decay curves

Sample	τ_1 (ns)	A_1 (%)	τ_2 (ns)	A_2 (%)	$\tau_{average}$ (ns)
$CsPbBr_3$ QDs	5.22	28.09	27.52	71.91	21.26
0.1 PEABr	5.04	28.26	25.23	71.74	19.60
0.3 PEABr	3.63	37.35	13.03	62.65	9.52
0.3 PEABr (505 nm) after reaction	2.36	88.57	17.01	11.43	4.03
0.5 PEABr (508 nm)	2.48	36.84	15.99	63.16	11.01
0.5 PEABr (438 nm)	1.80	96.59	11.80	3.41	2.14
0.5 PEABr (483 nm) after reaction	1.53	77.93	10.22	22.07	3.45
$(PEA)_2PbBr_4$	2.01	92.57	10.48	7.43	2.64

Table S2 Composition analysis of 0.3 PEABr and 0.5 PEABr sample before and after photocatalysis based on XPS spectra.

0.3 PEABr before catalysis	Peak Area	ASF	Area/ASF	Pb:Cs	Br:Pb
Cs 3d	87718.82	7.2	12183.17		
Pb 4f	88157.39	6.7	13157.82	**1.08**	**3.14**
Br 3d	34291.91	0.83	41315.56		
0.3 PEABr after catalysis	Peak Area	ASF	Area/ASF	Pb:Cs	Br:Pb
Cs 3d	39046.68	7.2	5423.15		
Pb 4f	53103.53	6.7	7375.49	**1.36**	**2.89**
Br 3d	17691.58	0.83	21315.16		
0.3 PEABr before catalysis	Peak Area	ASF	Area/ASF	Pb:Cs	Br:Pb
Cs 3d	61679.23	7.2	8566.56		
Pb 4f	64283.42	6.7	9594.54	**1.12**	**3.21**
Br 3d	25562.76	0.83	30798.50		
0.3 PEABr before catalysis	Peak Area	ASF	Area/ASF	Pb:Cs	Br:Pb
Cs 3d	13362.55	7.2	1855.91		
Pb 4f	23501.46	6.7	3507.68	**1.89**	**2.65**
Br 3d	7715.13	0.83	9295.34		

ASF: Atomic sensitivity factor

Table S3 Summary of relevant works on $CsPbBr_3$ QDs as photocatalysts for CO_2 reduction

Catalyst	Light	Condition	Product	$R_{electron}$ ($\mu molg^{-1}h^{-1}$)	Refs
0.3 PEABr	150 mW cm^{-2} AM 1.5G filter	H_2O Vapor	CO	30.0	This work
$CsPbBr_3$@ZIF	150 mW cm^{-2} AM 1.5G filter	H_2O Vapor	CO, CH_4	29.6	S1
α-Fe_2O_3/RGO/$CsPbBr_3$	150 mW cm^{-2} AM 1.5G filter	H_2O Vapor	CO, CH_4, H_2	81.0	S2
$CsPbBr_3$ QDs/PbS	150 mW cm^{-2} AM 1.5G filter	Ethyl acetate/water	CO, CH4	33.58	S3
$CsPbBr_3$ NC/Pd NS	150 mW cm^{-2} >420 nm	H_2O Vapor	CO, CH_4, H_2	33.8	S4
$CsPbBr_3$/BZNW/MRGO	150 mW cm^{-2} >420 nm	H_2O Vapor	CO, CH_4	52.0	S5
Fe: $CsPbBr_3$	150 mW cm^{-2}	H_2O Vapor	CO, CH_4	55.0	S6
$CsPbBr_3$@GDY-Co	100 mW cm^{-2} >400 nm	Acetonitrile/water	CO	55.4	S7
$CsPbBr_3$/Cs_4PbBr_6	100 mW cm^{-2} >400 nm	Deionized water	CO, CH_4	24.7	S8
$CsPbBr_3$ NCs (glycine)	100 mW/cm^{-2} >400 nm	H_2O Vapor	CO	55.4	S9
TiO_2/$CsPbBr_3$	300 W Xe lamp	Acetonitrile/water	CO, H_2	9.02	S10
P-CN/$CsPbBr_3$	300 W Xe lamp	Deionized water	CO	12.16	S11

References

S1 Z. C. Kong, J. F. Liao, Y. J. Dong, Y. F. Xu, H. Y. Chen, D. Bin Kuang and C. Y. Su, *ACS Energy Lett.*, 2018, **3**, 2656–2662.

S2 Y. Jiang, J. F. Liao, H. Y. Chen, H. H. Zhang, J. Y. Li, X. D. Wang and D. Bin Kuang, *Chem*, 2020, **6**, 766–780.

S3 J. Hu, M. Yang, X. Ke, S. Yang, K. Wang, H. Huang, W. Wang, D. Luo, Z. Zheng, L. Huang, P. Xiao, C. Tu, Y. Min, N. Huo and M. Zhang, *J. Power Sources*, 2021, **481**, 1–6.

S4 Y. F. Xu, M. Z. Yang, H. Y. Chen, J. F. Liao, X. D. Wang and D. Bin Kuang, *ACS Appl. Energy Mater.*, 2018, **1**, 5083–5089.

S5 Y. Jiang, J. F. Liao, Y. F. Xu, H. Y. Chen, X. D. Wang and D. Bin Kuang, *J. Mater. Chem. A*, 2019, **7**, 13762–13769.

S6 S. Shyamal, S. K. Dutta and N. Pradhan, *J. Phys. Chem. Lett.*, 2019, **10**, 7965–7969.

S7 K. Su, G. X. Dong, W. Zhang, Z. L. Liu, M. Zhang and T. B. Lu, *ACS Appl. Mater. Interfaces*, 2020, **12**, 50464–50471.

S8 Y. F. Mu, W. Zhang, X. X. Guo, G. X. Dong, M. Zhang and T. B. Lu, *ChemSusChem*, 2019, **12**, 4769–4774.

S9 Y. Xu, W. Zhang, K. Su, Y. X. Feng, Y. F. Mu, M. Zhang and T. B. Lu, *Chem. Eur. J.*, 2021, **27**, 2305–2309.

S10 F. Xu, K. Meng, B. Cheng, S. Wang, J. Xu and J. Yu, *Nat. Commun.*, 2020, **11**, 4613.

S11 Y. Wang, Z. Liu, X. Tang, P. Huo, Z. Zhu, B. Yang and Z. Liu, *New J. Chem.*, 2021, **45**, 1082–1091.